Taylor & Francis
Taylor & Francis Group

Trends in vegetation activity and their climatic correlates: China 1982 to 1998

JINGFENG XIAO* and A. MOODY

Department of Geography, University of North Carolina at Chapel Hill, Chapel Hill, North Carolina 27599-3220, USA

Abstract. We combined a satellite-derived Leaf Area Index (LAI) dataset and a gridded climate dataset to analyse trends in vegetation activity and their correlation with climate variability in China between 1982 and 1998. Vegetation activity over the growing season increased 11.03% in China during the 17-year period, which is broadly consistent with the greening trend in the northern high latitudes in Eurasia and North America shown in previous studies. Approximately 99×10^6 ha of croplands and 35×10^6 ha of forest exhibited significant upward trends in growing season LAI, and accounted for 53% and 19% of the total vegetated area with greening trends, respectively. Temperature was the leading climatic factor controlling greening patterns. However, trends in agricultural practices, such as increased use of high-yield crops and application of chemical fertilizers, along with land-use changes such as afforestation and reforestation probably made a greater contribution to the greening trend than temperature. Increased vegetation activity in forests suggests an increasing carbon stock in forest biomass in China, which supports previous studies based on satellite sensor data and forest inventory data.

1. Introduction

Terrestrial vegetation plays a large role in regulating the atmospheric CO_2 concentration through processes of photosynthesis, autotrophic respiration, and biomass combustion (Tans *et al.* 1990, Schimel *et al.* 1996). For example, recent studies have demonstrated that vegetation in the northern middle and high latitudes provides a large terrestrial carbon sink (Caspersen *et al.* 2000, Schimel *et al.* 2001). In addition, several studies have identified linear increases in vegetation activity during the past two decades (Myneni *et al.* 1997a, Zhou *et al.* 2001, Tucker *et al.* 2001, Bogaert *et al.* 2002, Lucht *et al.* 2002, Slayback *et al.* 2003) especially in the northern high latitudes of Eurasia and North America between $40°$ N and $70°$ N. Increases in spring temperatures are most likely driving these high-latitude trends, but changes in vegetation activity can also result from a variety of other factors, including other patterns of climate change (Tian *et al.* 1998, Schimel *et al.* 2000, Nemani *et al.* 2002), CO_2 fertilization (DeLucia *et al.* 1999, Schimel *et al.* 2000),

---

*Corresponding author; e-mail: jfxiao@email.unc.edu

nitrogen deposition (Nadelhoffer *et al.* 1999), fire suppression (Houghton *et al.* 2000), and land-use change (Houghton *et al.* 1999, Caspersen *et al.* 2000).

In China, as in other regions, observed increases in temperature and precipitation (Zhai *et al.* 1999, Shen and Varis 2001, IPCC 2001) may be driving changes in vegetation activity. For example, increases in warmth and moisture can amplify primary productivity by lengthening the period of carbon uptake (Nemani *et al.* 2002), enhancing photosynthesis (Keeling *et al.* 1996, Randerson *et al.* 1999), and improving nutrient availability by accelerating decomposition or mineralization (Melillo *et al.* 1993). Understanding the trends of vegetation activity in China and their responses to climate variability will help improve our understanding of the role of Chinese ecosystems in the global carbon cycle and global climate change.

In this paper, we present an analysis of the linear trends of vegetation activity and their associations with climate variability in China for all vegetated pixels, and for each vegetation type, between 1982 and 1998. This study is possible due to the availability of a global Leaf Area Index (LAI) dataset that has been retrieved from recently reprocessed Advanced Very High Resolution Radiometer (AVHRR) Normalized Difference Vegetation Index (NDVI) data (Myneni *et al.* 1997b, Nemani *et al.* 2003) and a global climatology dataset (New *et al.* 2000) both spanning the 17-year period.

2. Background

The AVHRR provides global vegetation observations with spatially and temporally consistent coverage from 1982 to present. The NDVI datasets derived from these data have been widely used to characterize vegetation activity at regional to global scales (Asrar *et al.* 1984, Myneni *et al.* 1995, Tucker *et al.* 2001, Zhou *et al.* 2001). However, calibration uncertainties, orbital drift, inter-sensor variability, bi-directional effects, and atmospheric effects, including volcanic eruptions, can all introduce noise to the spectral data, potentially generating faulty conclusions regarding apparent trends (Gutman 1999, Kaufmann *et al.* 2000, Zhou *et al.* 2001). The recently developed Version 3 Pathfinder NDVI dataset (Myneni *et al.* 1997b, Nemani *et al.* 2003) has been reprocessed and substantially improved from the earlier Pathfinder NDVI dataset (James and Kalluri 1994), and remaining sources of noise have been reduced. We used an LAI dataset retrieved from the Version 3 Pathfinder NDVI data to characterize vegetation activity (Myneni *et al.* 1997b).

Analyses of long-term NDVI observations indicate vegetation greening in the northern high latitudes (40° N–70° N) over the past two decades (Myneni *et al.* 1997a, Zhou *et al.* 2001, Tucker *et al.* 2001, Bogaert *et al.* 2002, Slayback *et al.* 2003). These findings have been corroborated by ground-based, phenological studies (Colombo 1998, Cayan *et al.* 2001, Fitter and Fitter 2002), climate-driven biogeochemical models (Lucht *et al.* 2002), and measured increases in carbon stock of woody biomass in these regions (Fan *et al.* 1998, Myneni *et al.* 2001, Schimel *et al.* 2001, Goodale *et al.* 2002). The greening trend corresponds with a pronounced warming, especially during winter and spring over Alaska, northern Canada, and northern Eurasia (Hansen *et al.* 1999) and has typically been attributed to an early onset of the growing season (Zhou *et al.* 2001, Tucker *et al.* 2001, Bogaert *et al.* 2002, Lucht *et al.* 2002). Precipitation has been assumed to play a minor role in increasing vegetation activity and has thus received less attention.

Although climate variability in China has been fairly well documented (Zhai *et al.* 1999, IPCC 2001, Shen and Varis 2001) trends of vegetation activity in China have received little focus relative to other regions. In addition to variability in

climate, China has undergone substantial changes in land use/land cover during the past two decades (World Resources Institute 1994, Ministry of Land and Resources of China 2002), which may contribute substantially to trends in vegetation activity. For example, forest inventory data have shown an increased carbon stock in forest biomass in China, mainly due to afforestation and reforestation (Goodale *et al.* 2002).

NDVI is closely related to the fraction of photosynthetically active radiation (fPAR) absorbed by vegetation canopies, and thus has often been used as a proxy for terrestrial photosynthetic activity (Asrar *et al.* 1984, Myneni *et al.* 1995). However, leaf and canopy processes that govern gas and energy exchange between vegetation and the atmosphere are better characterized by LAI particularly in dense canopies (Myneni *et al.* 1997b, Buermann *et al.* 2002). LAI is generally defined as one-sided green leaf area per unit ground area for broadleaf canopies, and projected needle leaf area per unit ground area in needle-leaf canopies (Myneni *et al.* 1997b, Buermann *et al.* 2002). We used satellite-retrieved LAI data in our analysis of trends in photosynthetic activity in China.

3. Data and methods

3.1. *Data*

3.1.1. *Satellite-derived LAI data*

The LAI dataset used for our analysis was produced using a radiative transfer model and the Version 3 Pathfinder NDVI dataset (Myneni *et al.* 1997b, Nemani *et al.* 2003). These data are gridded at 16 km spatial resolution and binned at monthly intervals. The original Pathfinder NDVI dataset (James and Kalluri 1994) was derived from AVHRR on board the National Oceanic and Atmospheric Administration's (NOAA) series of polar-orbiting meteorological satellites (NOAA 7, 9, 11 and 14). Data processing included improved navigation, cloud masking, sensor calibration, and partial correction for Rayleigh scattering (James and Kalluri 1994).

In the Version 3 Pathfinder NDVI dataset, remaining noise associated with residual atmospheric effects, orbital drift effects, inter-sensor variations, and stratospheric aerosol effects (Myneni *et al.* 1998, Kaufmann *et al.* 2000) was further reduced by a series of corrections, including temporal compositing, spatial compositing, orbital correction, and climate correction (Nemani *et al.* 2003). This reprocessed NDVI dataset was then used to create the 16 km monthly LAI dataset using a three-dimensional radiative transfer model and a land-cover map as described in Myneni *et al.* (1997b).

3.1.2. *Climatology data*

We used a global monthly climatology dataset, interpolated from station observations, and gridded at 0.5° resolution (New *et al.* 2000). This dataset includes seven climate variables: precipitation, mean temperature, diurnal temperature range, wet-day frequency, vapour pressure, cloud cover, and ground frost frequency. We used two variables, precipitation and temperature. This dataset has higher spatial resolution, longer temporal coverage, and more strict temporal fidelity than other climatology datasets (New *et al.* 2000).

3.1.3. *Land-cover map*

We used the 2001 land-cover map (Friedl *et al.* 2002) derived from Moderate Resolution Imaging Spectroradiometer (MODIS) data to identify vegetated pixels by land-cover type. This land-cover map has 1 km spatial resolution, and identifies 13 land-cover types (table 1, figure 1). All vegetation types except Savanna were considered in this analysis.

3.2. *Methods*

To match the 16 km LAI dataset, the monthly precipitation and temperature data from 1982 to 1998 were resampled to 16 km resolution. The 1 km MODIS land-cover map was aggregated to 16 km resolution using a plurality rule. That is, each 16 km grid cell was labelled according to the most commonly occurring cover type among its constituent 1 km pixels. All data were projected to the Lambert Azimuthal Equal-Area map projection, and co-registered in a geographical information system (GIS).

We generated spatially averaged time series of mean LAI, mean temperature, and total precipitation over the growing season (April–October) for all vegetated pixels, and for each vegetation type. The linear time trend in each LAI time series was estimated by regressing LAI as a function of time over the study period, following Zhou *et al.* (2001). We then analysed the correlations between LAI and climate data to assess the associations between vegetation activity and climate variability. These analyses were repeated for spring (March–May), summer (June–August), autumn (September–November), and winter (December–February). A *p*-value of 0.05 was used as the test criteria for significance of all correlation statistics.

Since spatial averaging hides the geographical variability of LAI, we also analysed the spatial patterns of LAI trends on a per-pixel basis. We identified all vegetated pixels with linear trends in LAI that were statistically significant over the 17-year period. For these pixels, we further analysed the correlations between LAI and climate variables. These analyses were repeated for each season. The relative

Table 1. The total number of pixels within each vegetation type and its percentage and area in China based on the 2001 MODIS land-cover map (Friedl *et al.* 2002).

| Vegetation type	Number of pixels	Per cent (%)	Area ($\times 10^6$ ha)
Evergreen Needleleaf Forest (ENF)	146	0.40	3.74
Evergreen Broadleaf Forest (EBF)	560	1.53	14.34
Deciduous Needleleaf Forest (DNF)	24	0.07	0.61
Deciduous Broadleaf Forest (DBF)	175	0.48	4.48
Mixed Forest (MF)	3946	10.75	101.02
Subtotal (forests)	(4851)	(13.21)	(124.19)
Closed Shrubland (CSH)	266	0.72	6.81
Open Shrubland (OSH)	6711	18.28	171.80
Woody Savanna (WS)	1069	2.91	27.37
Savanna (Sa)	2	0.01	0.05
Grassland (Gr)	5632	15.34	144.18
Cropland (Cr)	10443	28.44	267.34
Barren or Sparsely Vegetated (Barren)	7743	21.09	198.22
Water	334	0.91	8.55
Total	37051	100	948.51
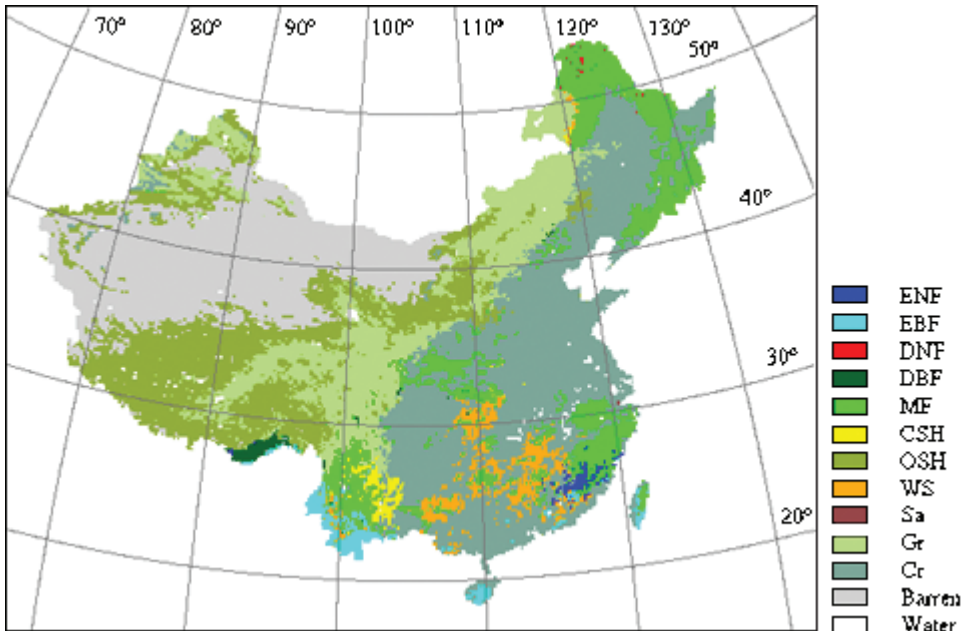
Figure 1.   The distribution of land-cover types in China, based on the 2001 MODIS land-cover map (Friedl *et al*. 2002). China was divided into seven geographical regions, based on climate, topography, vegetation, land use and social economy: northern (1), north-eastern (2), north-western (3), middle (4), eastern (5), south-western (6), and southern (7). Longitudes (west of Greenwich) and latitudes (north of equator) are shown at 10° intervals. ENF, Evergreen Needleleaf Forest; EBF, Evergreen Broadleaf Forest; DNF, Deciduous Needleleaf Forest; DBF, Deciduous Broadleaf Forest; MF, Mixed Forest; CSH, Closed Shrubland; OSH, Open Shrubland; WS, Woody Savanna; Gr, Grassland; Cr, Cropland; All, All vegetated pixels.

strength of significant trends in LAI, and significant correlations between LAI and climate variables were mapped and evaluated.

4.   Results

4.1. *Trends in spatially averaged LAI*

4.1.1. *Growing season LAI*

The spatially averaged time series of growing season LAI (LAIg) for all vegetated pixels exhibited a significant upward trend, with an increase of 11.03% between 1982 and 1998 (table 2, figure 2(*a*)). At the coarse scale considered, there were no significant correlations between LAI and temperature or precipitation over the 17-year period.

LAIg also exhibited significant upward trends for each vegetation type except Evergreen Needleleaf Forest, Evergreen Broadleaf Forest, Closed Shrubland, and Grassland (table 2). The magnitudes of LAIg trends varied by vegetation type, from 6.72 to 15.16% for Mixed Forest and Cropland, respectively. Noticeably, the temporal pattern of LAIg for Cropland is similar to the overall pattern for all vegetated pixels pooled together (figure 2). There were significant correlations between LAIg and temperature for Deciduous Needleleaf Forest (figure 3(*a*)) and between LAIg and precipitation for Open Shrubland (figure 3(*b*)).

Table 2. Linear trends of spatially averaged time series of growing season LAI (LAIg) for all vegetated pixels and within each vegetation type (0.05 significance level).

Vegetation type	Changes in growing season LAI averages during 17 years (1982–1998)			
	Absolute values	Per cent (%)	r^2	*p* value
Evergreen Needleleaf Forest	0.172	3.36	0.16	0.12
Evergreen Broadleaf Forest	0.301	6.26	0.20	0.07
Deciduous Needleleaf Forest	0.539	11.27	0.51	0.0014
Deciduous Broadleaf Forest	0.394	8.15	0.37	0.009
Mixed Forest	0.314	6.72	0.46	0.0027
Closed Shrubland	0.251	8.59	0.09	0.25
Open Shrubland	0.155	11.27	0.24	0.045
Woody Savanna	0.570	14.93	0.41	0.006
Grassland	0.146	6.95	0.18	0.09
Cropland	0.381	15.16	0.44	0.038
All vegetated pixels	0.308	11.03	0.43	0.004

4.1.2. *Seasonal LAI*

Averaged over all vegetated pixels, spring LAI showed a significant upward trend over the 17-year period (table 3, figure 4(*a*)). In addition, there was a significant correlation between spring LAI and spring temperature over the 17-year period (figure 5(*h*)). There was no significant correlation between spring LAI and spring precipitation. No significant trends in LAI were observed over any other season.

Spring LAI exhibited a significant upward trend for each individual vegetation type (table 3). The magnitude of trends in spring LAI varied by vegetation type from 20.91 to 48.34%, for Evergreen Needleleaf Forest and Woody Savanna, respectively (table 3). Evergreen Needleleaf Forest showed a significant upward trend in spring LAI but not in LAIg, suggesting its trend in productivity is primarily attributed to spring rather than the whole growing season. Again, the temporal pattern of spring LAI for Cropland reflected the overall pattern for all vegetated pixels (figure 4). There was a significant correlation between spring LAI and spring temperature for all classes except Deciduous Broadleaf Forest and the two shrubland classes (figure 5). There was no significant correlation between spring LAI and spring precipitation for any vegetation type.

For Evergreen Broadleaf Forest, summer LAI exhibited a significant downward trend from 1982 to 1998, with an overall reduction of 6.68%. No significant trend in summer LAI was observed for any other vegetation type. Autumn LAI increased by 4.13% for Deciduous Broadleaf Forest. Winter LAI exhibited significant upward trends for Evergreen Needleleaf Forest, Evergreen Broadleaf Forest and Mixed Forest, with an increase of 7.02%, 6.59% and 16.35%, respectively. There was a significant correlation between winter LAI and winter temperature for Evergreen Broadleaf Forest (figure 6(*a*)) and Mixed Forest (figure 6(*b*)).

4.2. *Spatial patterns of LAI trends and climatic effects*
4.2.1. *Spatial patterns of LAI trends*

Over the entire country, 25.14% of the vegetated pixels exhibited significant upward trends in LAIg from 1982 to 1998 (table 4, figure 7(*a*)). The greening trend
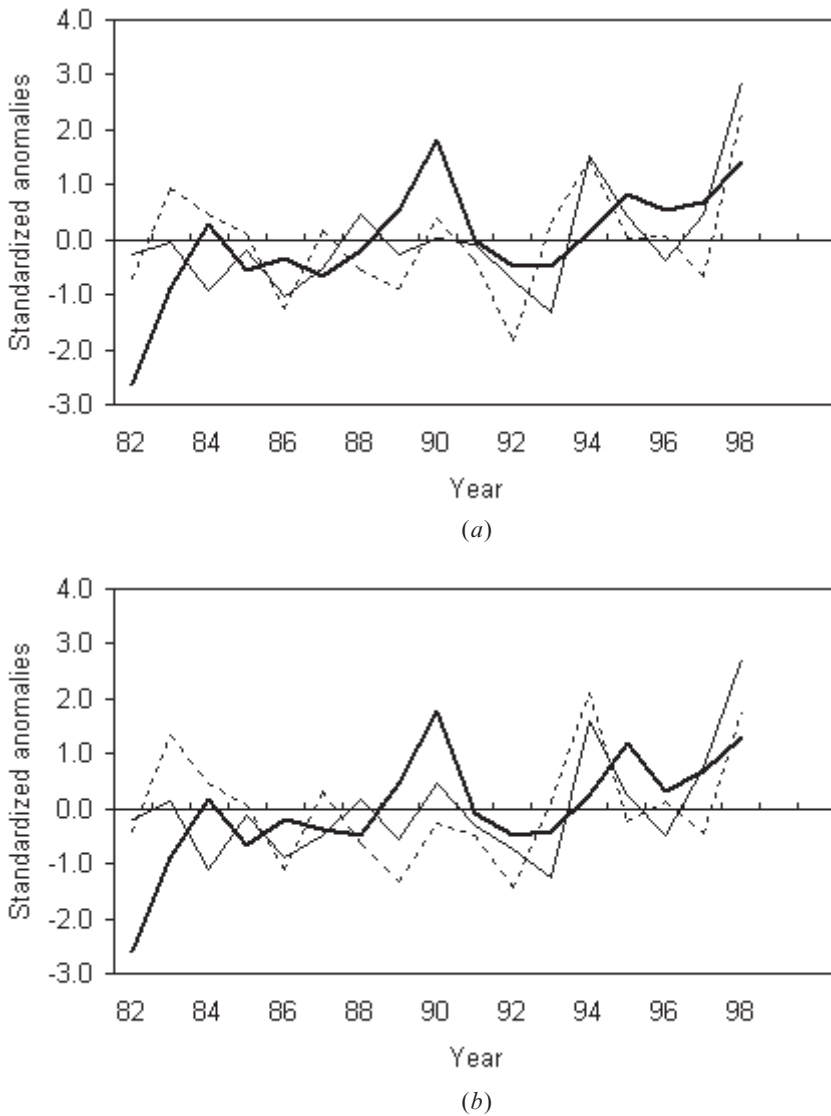
Figure 2. Spatially averaged time series of growing season LAI (heavy solid line), mean
temperature (light solid line), and total precipitation (dashed line) for the period
1982–1998: (*a*) All vegetated pixels; (*b*) Cropland.

was observed over a swath of land from north-eastern and northern China through
middle and eastern China to southern China. A greening pattern was also observed
in the westernmost portion of the country. A downward trend in LAI was observed
only in the middle of north-western China.

The percentages of pixels with positive LAI trends varied substantially by
vegetation type, ranging from 8.90 to 66.67% for Evergreen Needleleaf Forest and
Deciduous Needleleaf Forest, respectively (table 4).

The total area of vegetated pixels that exhibited trends in LAI varied by
vegetation type (table 4). Cropland, the three forest classes combined, and
Grassland accounted for 53%, 18.7%, and 12.4% of the total vegetated area with
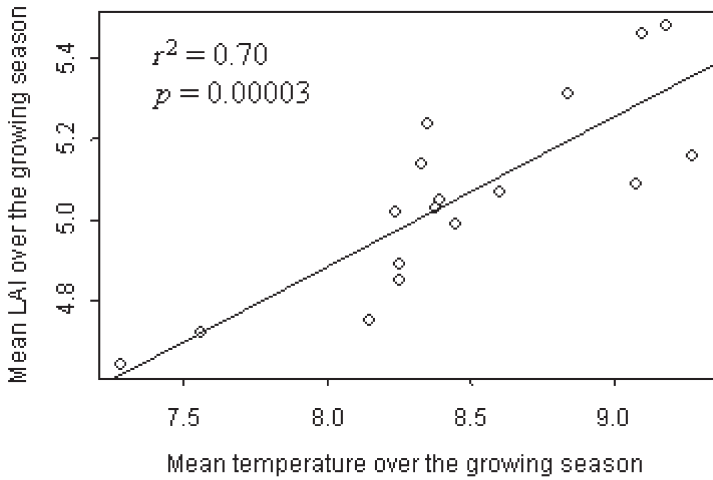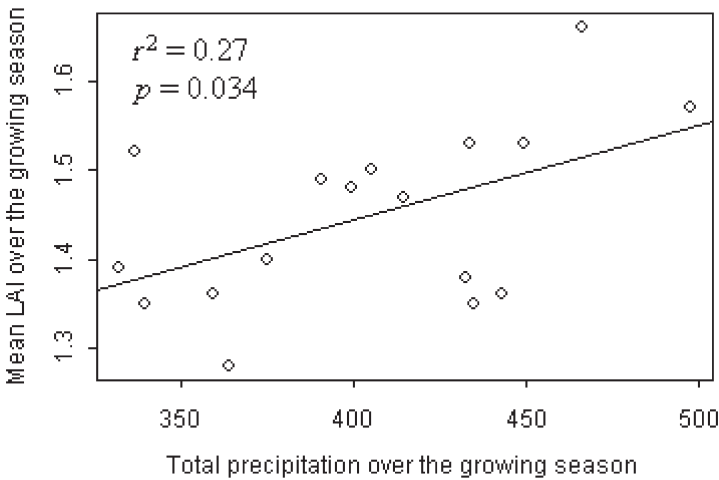
Figure 3.   Relationships between growing season LAI and growing season climate variables
from 1982 to 1998. (*a*) LAI and temperature for Deciduous Needleleaf Forest; (*b*)
LAI and precipitation for Open Shrubland.

upward LAI trends. Of the total area classified as Cropland, 37% had positive
trends in LAI. Positive trends occurred for 28% of forested pixels and 16% of the
total grassland area.

   The greening pattern over the entire country varied considerably by season
(table 4, figure 7(*b*)–(*e*), figure 8). In spring, 28% of all vegetated pixels showed
positive trends in LAI. These areas were mainly located in the southern portion of
northern China, the northern portion of eastern China, and portions of the south-
western, middle, and southern regions. In summer, autumn and winter, LAI
increased for 10.5%, 12.3% and 12.2% of pixels, respectively (table 4).

   The greening pattern in spring is more prevalent than in any other season. The
area of pixels with upward trends in spring LAI varied by vegetation type (table 4).

Table 3. Linear trends of spatially averaged time series of spring LAI for all vegetated pixels and within each vegetation type (1982–1998).

Vegetation type	Changes in growing season LAI averages during 17 years			
	Absolute values	Per cent (%)	r^2	p value
Evergreen Needleleaf Forest	0.847	20.91	0.40	0.007
Evergreen Broadleaf Forest	0.890	22.86	0.76	0.000005
Deciduous Needleleaf Forest	0.669	30.92	0.25	0.041
Deciduous Broadleaf Forest	0.895	23.40	0.42	0.005
Mixed Forest	0.691	26.18	0.52	0.001
Closed Shrubland	0.611	39.57	0.57	0.0005
Open Shrubland	0.135	32.12	0.43	0.004
Woody Savanna	0.911	48.34	0.53	0.0009
Grassland	0.218	32.13	0.43	0.004
Cropland	0.485	42.12	0.52	0.001
All vegetated pixels	0.456	33.63	0.57	0.0005

Increases in LAI accounted for 39.5%, 37.9%, and 17.9% of the total area of Cropland, all forest classes, and Grassland, respectively. These areas accounted for 50.7%, 22.6%, and 12.4% of the total vegetated area, respectively.

4.2.2. *Climatic effects on LAI trends*

For all vegetated pixels with significant upward trends in LAIg, 19.92% exhibited positive LAI–temperature correlations, mainly distributed in the north-ernmost portion of China and middle China (figure 8(*k*), figure 9(*a*)). For cropland and forested areas, 15.75% and 42.5% of those pixels with upward LAIg trends exhibited positive LAI–temperature correlations, respectively (figures 8 and 9). Low percentages of pixels showed significant LAI–precipitation correlations (figures 8 and 10), which may be attributable to chance since we used a 0.05 significance level throughout our analyses.

Taken together, 31.67% of those pixels with upward trends in spring LAI exhibited positive LAI–temperature correlations, mainly distributed over a swath of land from north-eastern China through middle China to southern China (figure 8(*k*), figure 9(*b*)). Positive LAI–temperature correlations were observed for 23.95%, 46.69% and 33.93% of cropland, forest and grassland pixels with upward trends in spring LAI, respectively (figures 8 and 9). Compared with temperature, precipitation plays a minor, if any, role in explaining the greening pattern (figures 8 and 10). Similarly, for any other season and most vegetation types, temperature makes a greater contribution to the greening pattern than precipitation does (figure 8).

5. Discussion

Our results indicate an 11.03% increase in growing season LAI in China between 1982 and 1998 (table 2). A recent study by Zhou *et al.* (2001) showed that vegetation activity increased by 12.41% and 8.44% in Eurasia and North America (40° N–70° N), respectively from 1982 to 1999. Thus, the magnitude of greening in China is in broad agreement with trends reported for the northern high latitudes.

Of all vegetated pixels, approximately 25% exhibited positive trends in growing season LAI (figures 7 and 8). The percentage of area with increased LAI varied
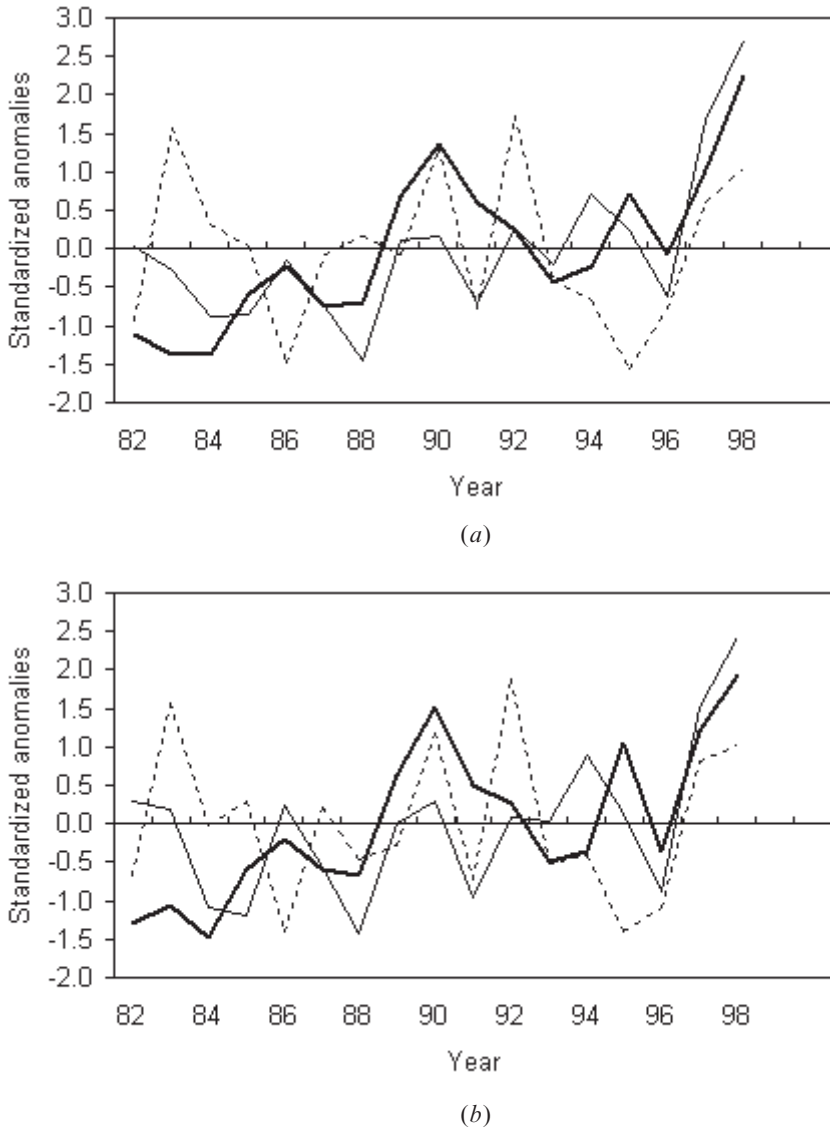
(a)

(b)

Figure 4.   Spatially averaged time series of spring LAI (heavy solid line), mean temperature (light solid line) and total precipitation (dashed line) for the period 1982–1998 for (a) All vegetated pixels and (b) Cropland.

considerably by vegetation type, but was particularly high for Deciduous Needleleaf Forest, Mixed Forest, Woody Savanna, and Cropland. The latter three classes contributed 76% to the total area undergoing greening. Grassland and Open Shrubland contributed an additional 21%. The significant trend in LAIg for Deciduous Needleleaf Forest was strongly correlated with temperature (figure 3). This is consistent with studies suggesting that productivity in northern high latitudes is increasing in response to elevated temperatures, especially during spring (Zhou *et al*. 2001, Tucker *et al*. 2001, Lucht *et al*. 2002).

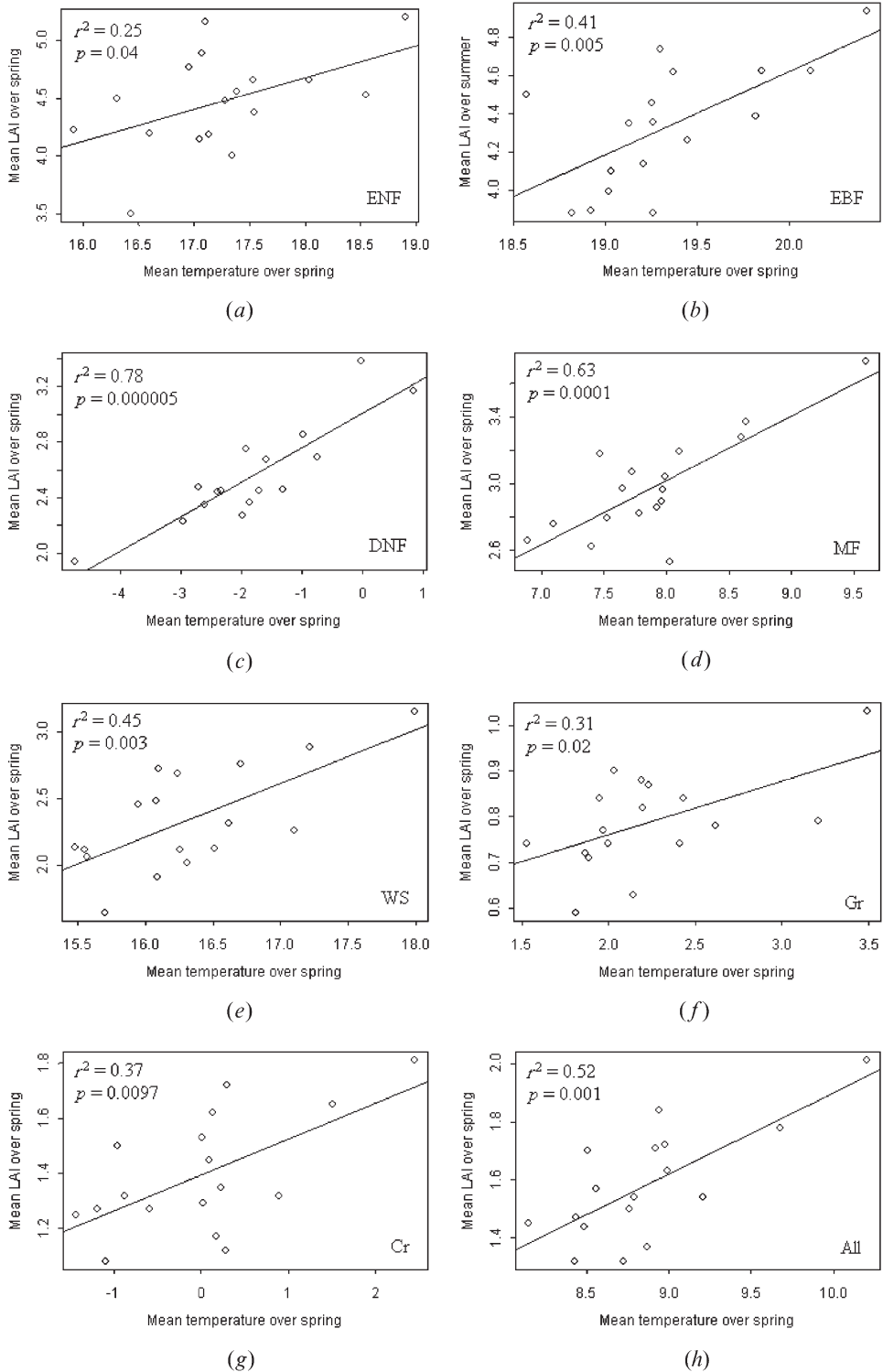All vegetation types exhibited increasing LAI in spring (table 3). Moreover, in

Figure 5. Relationships between spring LAI and spring temperature from 1982 to 1998 for (*a*) Evergreen Needleleaf Forest, (*b*) Evergreen Broadleaf Forest, (*c*) Deciduous Needleleaf Forest, (*d*) Mixed Forest, (*e*) Woody Savanna, (*f*) Grassland, (*g*) Cropland, and (*h*) All vegetated pixels.

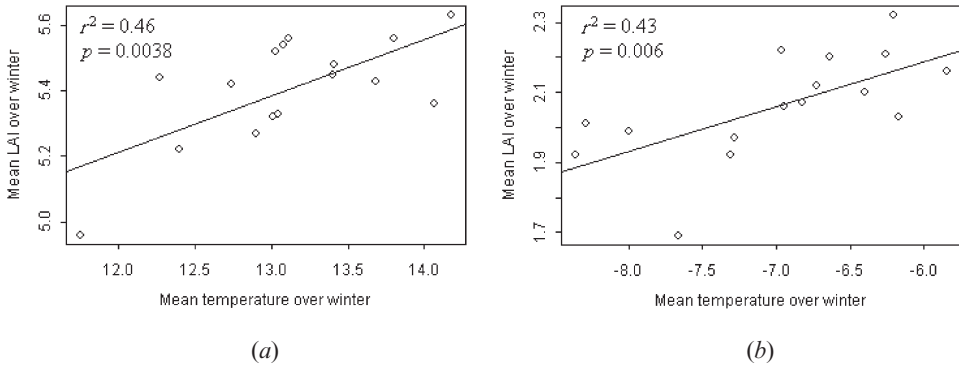(*a*)   (*b*)

Figure 6.   Relationships between winter LAI and winter temperature from 1982 to 1998 for
(*a*) Evergreen Broadleaf Forest and (*b*) Mixed Forest.

Table 4.   Percentages (%) and areas ($\times 10^6$ ha) of vegetated pixels with significant upward
trends ($p < 0.05$) in LAI for all vegetated pixels and within each vegetation type.

Vegetation type	Growing season		Spring		Summer		Autumn		Winter	
	Per cent	Area	Per cent	Area	Per cent	Area	Per cent	Area	Per cent	Area
ENF	8.90	0.33	39.04	1.46	0.68	0.03	0.00	0	17.81	0.67
EBF	19.46	2.79	51.25	7.35	5.00	0.72	5.89	0.84	17.32	2.48
DNF	66.67	0.41	25.00	0.15	0.00	0	20.83	0.13	20.83	0.13
DBF	20.57	0.92	29.71	1.33	5.71	0.26	5.71	0.26	10.86	0.49
MF	30.06	30.37	36.37	36.74	3.67	3.71	8.39	8.48	18.80	18.99
CSH	12.78	0.87	46.62	3.17	1.13	0.08	12.41	0.85	13.53	0.92
OSH	9.61	16.51	7.96	13.68	7.24	12.44	5.92	10.17	3.10	5.33
WS	43.87	12.01	47.05	12.88	10.76	2.94	11.41	3.12	5.05	1.38
Gr	16.03	23.11	17.90	25.81	9.98	14.39	10.35	14.92	11.95	17.23
Cr	37.08	99.13	39.51	105.63	16.25	43.44	19.75	52.8	15.89	42.48
All	25.14	186.45	28.07	208.19	10.52	78	12.34	91.56	12.15	90.09

ENF, Evergreen Needleleaf Forest; EBF, Evergreen Broadleaf Forest; DNF, Deciduous
Needleleaf Forest; DBF, Deciduous Broadleaf Forest; MF, Mixed Forest; CSH, Closed
Shrubland; OSH, Open Shrubland; WS, Woody Savanna; Gr, Grassland; Cr, Cropland; All,
All vegetated pixels.

almost every case, this trend was significantly correlated with spring temperature,
especially for Evergreen Needleleaf Forest and Mixed Forest (table 3, figure 5).
Significant increases in spring LAI occurred for 28% of the total land area, and for
half of this area, observed trends in LAI were significantly correlated with spring
temperatures. Thus, while not all vegetation types showed increases in LAI over the
growing season, and while other driving factors probably explain the bulk of the
greening trend in China, the results from spring suggest that there is an overall
enhancement of LAI in the early growing season, and that much of that
enhancement can be explained by increasing springtime temperatures. There also
appear to be winter warming effects for Mixed Forest and Evergreen Broadleaf
Forest, a vegetation type restricted to subtropical regions bordering Vietnam, Laos
and Myanmar (figure 6). Note that Open Shrubland was the only class to exhibit a
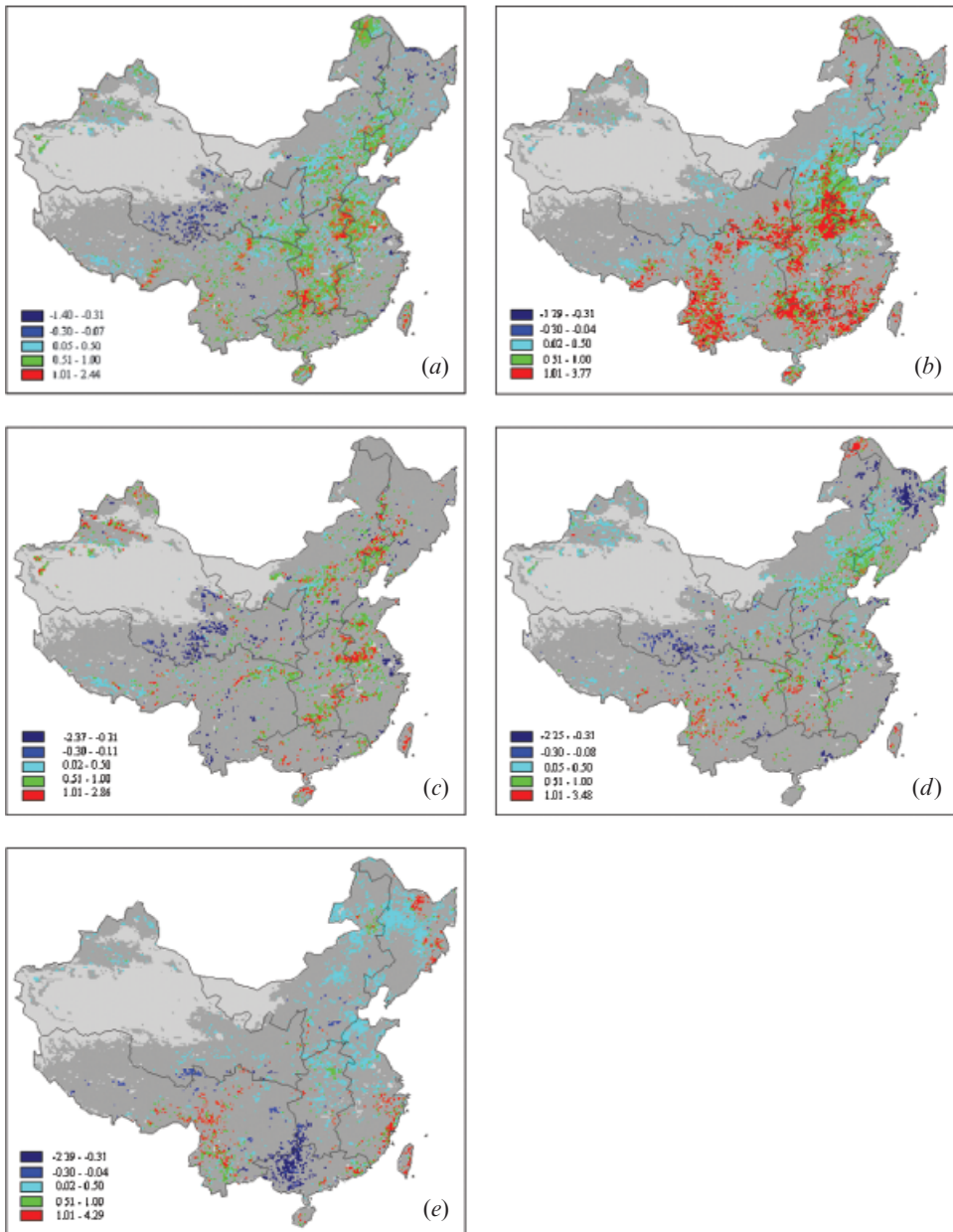trend in LAIg that was correlated with precipitation (figure 3(*b*)). Although this

Figure 7. Linear trends (LAI units per 17 years) of mean LAI in China from 1982 to 1998 on a per-pixel basis. Coloured areas indicate pixels with statistically significant ($p < 0.05$) trends in LAI. Dark grey areas indicate pixels with no significant trends in LAI. Light grey areas are classified as non-vegetated. (*a*) Growing season, (*b*) spring, (*c*) summer, (*d*) autumn, (*e*) winter.

effect was fairly weak, it is potentially indicative of woody thickening, such as that observed in other semi-arid regions of the world (Van Auken 2000).

There are large areas for which significant increases in LAIg were not explained by temperature or precipitation. For example, Cropland, which makes up 36% of

the total vegetated land area in China, accounted for roughly half of the total area that exhibited greening, but showed very little response to climate. The rise in crop management practices such as fertilization, irrigation, pest control, and resistant, high-yield crop varieties have undoubtedly enhanced the productivity of crops, and
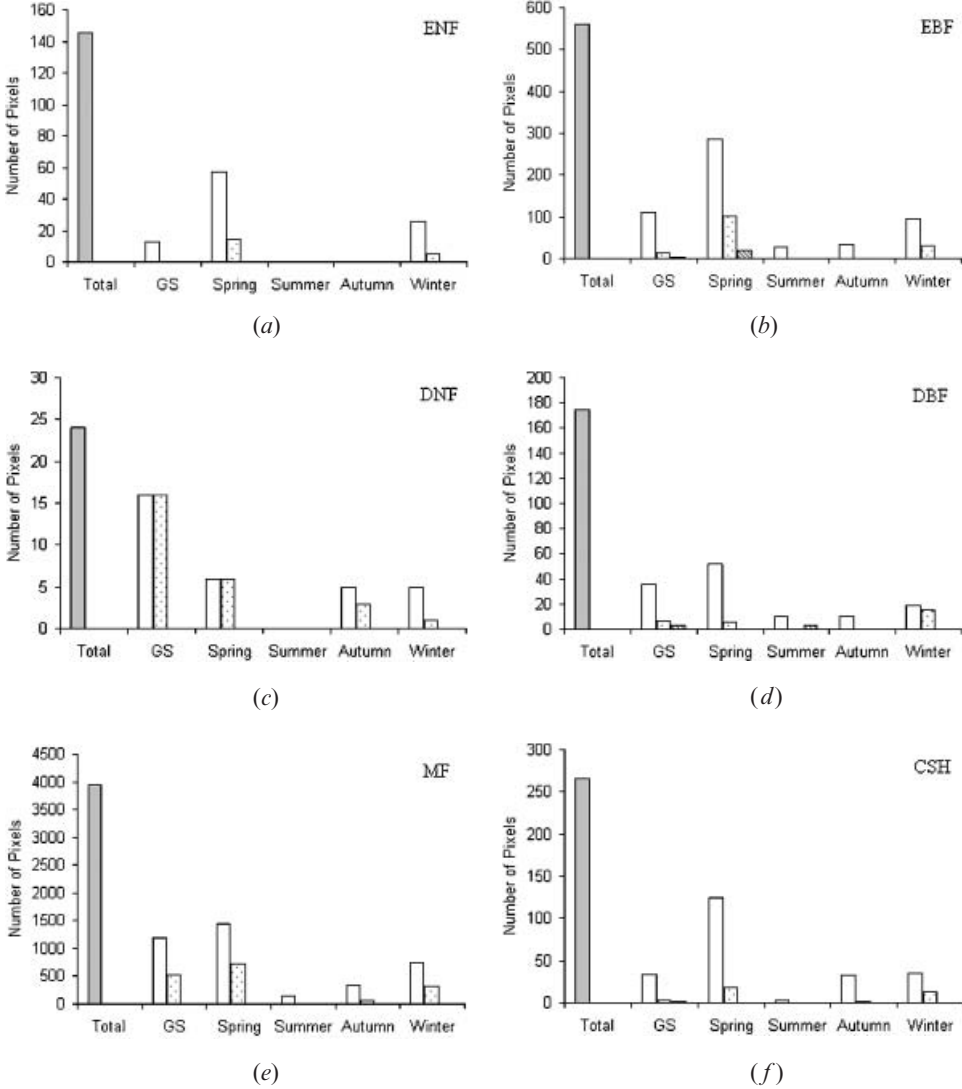

Figure 8. Total numbers of pixels, pixels with significant upward trends, and pixels with significant LAI–temperature and LAI–precipitation correlations for (*a*) Evergreen Needleleaf Forest, (*b*) Evergreen Broadleaf Forest, (*c*) Deciduous Needleleaf Forest, (*d*) Deciduous Broadleaf Forest, (*e*) Mixed Forest, (*f*) Closed Shrubland, (*g*) Open Shrubland, (*h*) Woody Savanna, (*i*) Grassland; (*j*) Cropland, and (*k*) All vegetated pixels. Grey bar indicates the total number of pixels. White bar indicates the total number of pixels with significant upward trends. Dotted bar indicates the total number of pixels with both significant upward trends and significant LAI–temperature correlations. Downward diagonal bar indicates the total number of pixels with both significant upward trends and LAI–precipitation correlations. GS, Growing season.
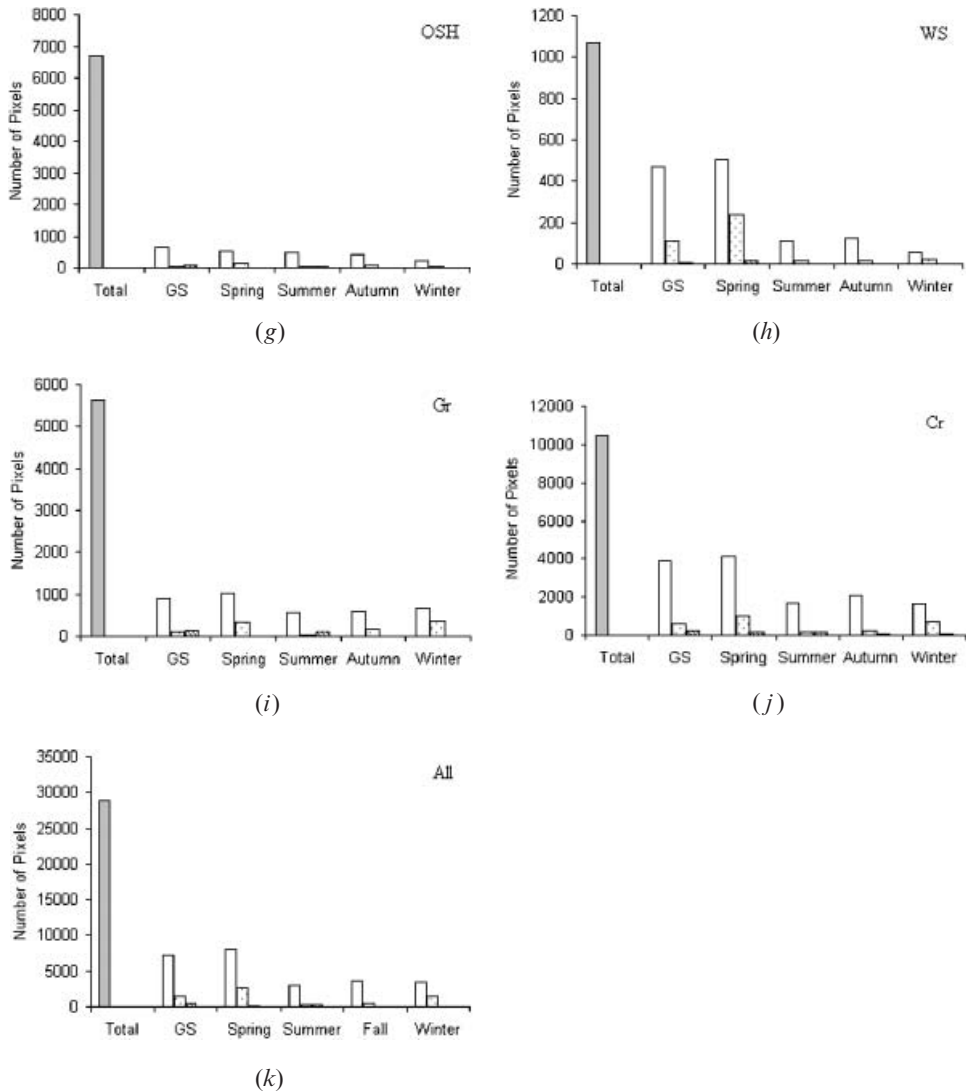
(g)

(h)

(i)

(j)

(k)

Figure 8.   (*Continued.*)

thus contributed to the greening trend in China. Based on historical data, Tong *et al.* (2003) reported that the yield per hectare for all crops has increased from $1.21\,t\,ha^{-1}$ in 1961 to $4.83\,t\,ha^{-1}$ in 1998, mainly due to the substitution of high-yield crops for low-yield crops and rapid increase of chemical fertilizer use.

A greening trend was observed over $34.8 \times 10^{6}\,ha$ of forested land. This accounted for 28% of the total forested area in China. Enhanced vegetation activity in Mixed Forest, by far the most prevalent forest type in China, suggests an increasing carbon stock in forest biomass. This is consistent with other studies based on NDVI (Myneni *et al.* 2001) and forest inventory data (Goodale *et al.* 2002) which show that Chinese forests are functioning as a terrestrial carbon sink. For nearly 50% of the forested area with increased LAIg, the greening trend was significantly correlated with elevated temperature over the growing season. This suggests that half of the observed greening pattern might be attributed to climate
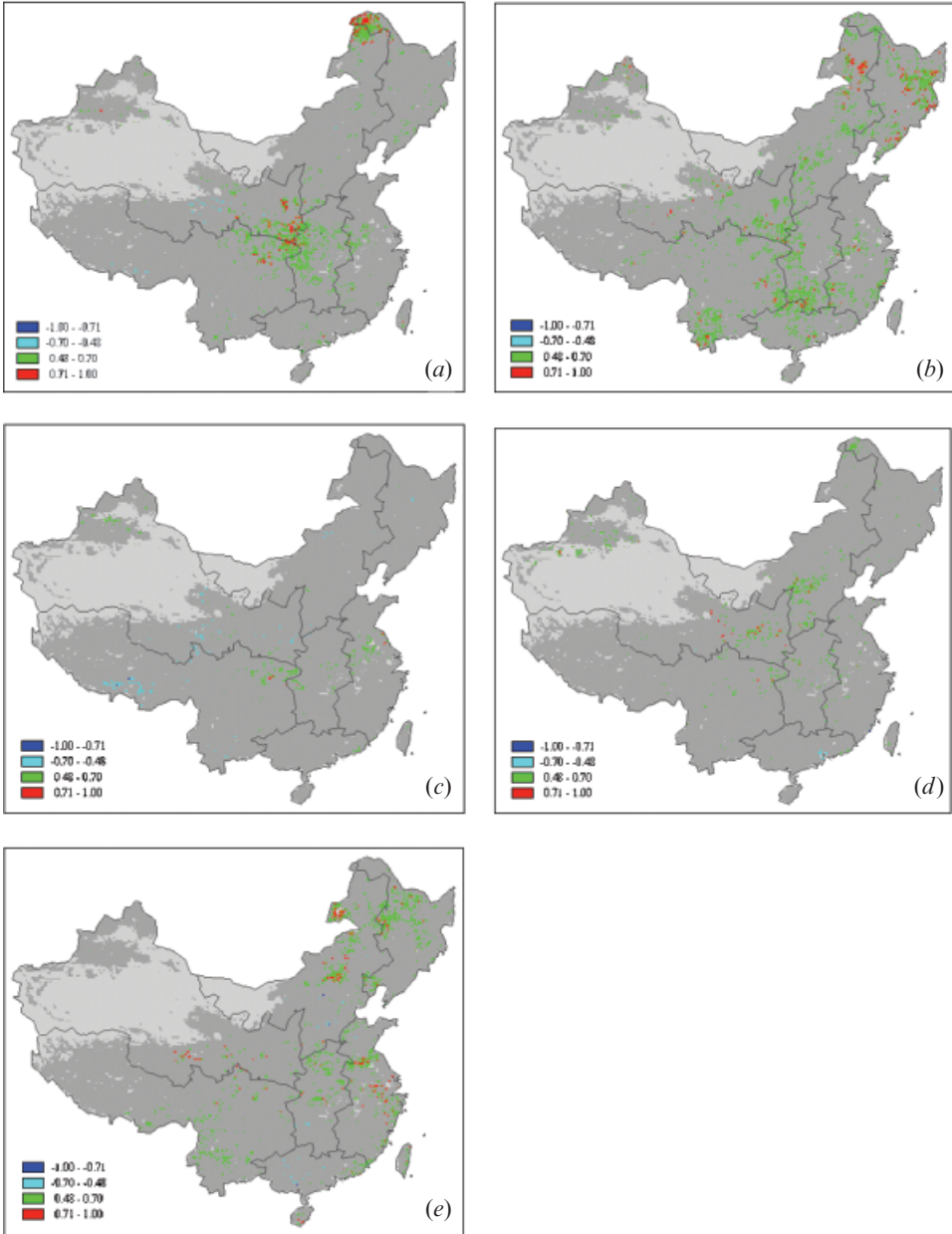
Figure 9. Correlation coefficients (*r*) of the relationship between LAI and temperature in China from 1982 to 1998 on a per-pixel basis. Coloured areas indicate those pixels with both statistically significant ($p < 0.05$) trends in LAI and statistically significant ($p < 0.05$) correlations between LAI and temperature. Dark grey areas indicate not only those pixels without significant trends in LAI but also those pixels with significant trends in LAI but with an absence of correlation between LAI and temperature. Light grey areas indicate non-vegetated pixels. (*a*) Growing season, (*b*) spring, (*c*) summer, (*d*) autumn, (*e*) winter.
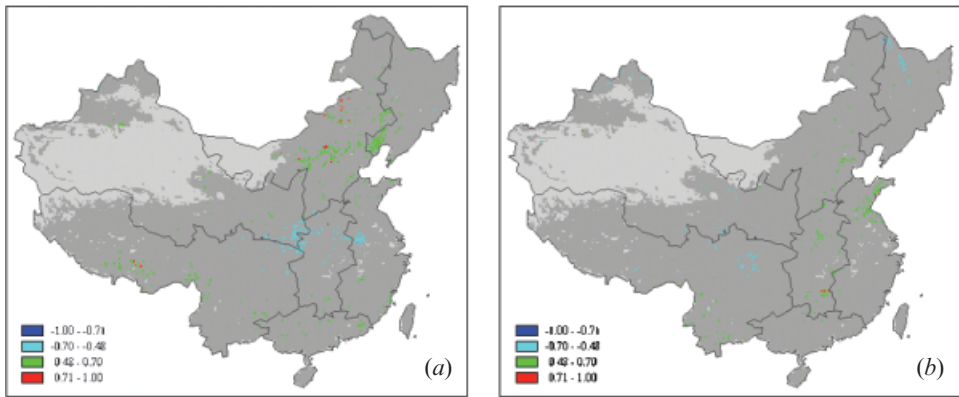
Figure 10. Correlation coefficients (*r*) between LAI and precipitation in China from 1982 to 1998 on a per-pixel basis. Interpretation as in figure 8. (*a*) Growing season, (*b*) spring.

change, and that the remainder is due to some other factors. It is most likely that afforestation and reforestation have contributed substantially to forest greening. According to Liu (1996) the total forested area in China has increased from 5.2% in 1950 to 13.9% in 1995, primarily due to the development of plantations in non-forested areas, although natural forests have substantially declined due to extensive cutting of forests and woody harvest (Zhang *et al.* 1999, 2000).

Chinese government documents state that a total of 57.97×10^6 ha plantation-style forests were planted during the 1980s, and 52.83×10^6 ha forests were planted during the 1990s (Chinese Ministry of Forestry 1987–1998, 1999–2001). Much of this plantation activity would have been in early growth stages in 2001, and thus, may not have been classified as forest in the MODIS land-cover map used here. For example, immature tree canopies may have been misclassified as Woody Savanna or Shrubland. In addition, the currently existing area of these more recent plantation-style forests might be well below the total area planted, because the mortality of planted trees was up to 65% before 1985 and 15% afterwards (Chinese Ministry of Forestry 1987–1998, 1999–2001).

Several geographic regions (figure 1) that exhibit strong trends in LAI require closer examination. For example, there is a concentration of pixels that exhibit negative trends in LAIg distributed throughout Grassland and Open Shrubland in Region 3, east of the Gobi Desert (figure 7). Productivity in this region would presumably be limited by soil moisture availability, however the observed trends in LAIg were not correlated with precipitation (or temperature). The concentrated area of increasing LAIg in far northern China is composed of Mixed Forest and Deciduous Needleleaf Forest. The subtropical area in the southernmost part of Region 6 is dominated by Evergreen Broadleaf Forest, Mixed Forest and Closed Shrubland, and exhibits a strong, spatially coherent increase in spring LAI (figure 7(*b*)), which is largely correlated with spring temperature (figure 9(*b*)). Geographically, the dominant temperature effect on LAIg is distributed in far northern China, and in the area where regions 1, 3, 4 and 6 converge. The latter area is dominated by Cropland, but also includes some Mixed Forest and Woody Savanna.

As with all studies of this type, there is a set of data uncertainties that requires consideration. Residual noise remaining in the Version 3 Pathfinder NDVI dataset

will lead to uncertainties in the resulting LAI dataset and hence in the magnitudes of LAI trends. We thus emphasize the general trends of LAI rather than the magnitudes. In addition, the MODIS land-cover map that was used to identify the class types of vegetated pixels undoubtedly contains both classification and aggregation error. Each grid cell in the aggregated map corresponds to 256 pixels in the 1 km land-cover map, and the label for each cell is based on a plurality rule. Since each aggregated grid cell represents an area of 2.56×10^4 ha, relatively uncommon classes, or classes that occur in a heterogeneous matrix were reduced in area in favour of larger, more homogeneous classes.

In addition to the data issues identified above, this study does not fully consider changes in land cover and land use over the study period. Thus, trends in LAI that resulted from such changes cannot be fully separated from trends due to climatic drivers. Finally, although we focused on the longest period (1982–1998) for which we had access to both satellite and climatology data, the 17-year period is a short record for studies of vegetation dynamics and climate variability. Hence, relatively extreme years in terms of climate or productivity may introduce bias to statistical assessments of the observed trends.

6.   Conclusions

We found an 11% increase in growing season LAI in China between 1982 and 1998. Cropland and forest accounted for the majority of this increase, probably reflecting trends in land use and land-management practices. However, there were notable increases in spring LAI that correlated strongly with increasing spring temperatures, suggesting a climate change impact on seasonal, if not annual, productivity. As in high latitudes elsewhere in the northern hemisphere, forested regions in northern China have exhibited increasing LAI, apparently in response to increasing temperatures. Increased vegetation activity in forested areas throughout China may reflect an increasing carbon stock in forest biomass (Myneni *et al*. 2001, Goodale *et al*. 2002). Twenty-five per cent of the entire vegetated area of China exhibited upward trends in LAIg. However, of these, only about 20% were correlated with temperature, and 7% with precipitation. Thus, observed changes in LAI result from the combined effects of land management and climate, with the former driving the bulk of these changes. Land management and climate change may interact in their joint effect on productivity and carbon dynamics, and these effects can vary substantially among vegetation types.

References

ASRAR, G., FUCHS, M., KANEMASU, E. T., and HATFIELD, J. L., 1984, Estimating absorbed photosynthetic radiation and leaf-area index from spectral reflectance in wheat. *Agronomy Journal*, **76**, 300–306.

BOGAERT, J., ZHOU, L., TUCKER, C. J., MYNENI, R. B., and CEULEMANS, R., 2002, Evidence for a persistent and extensive greening trend in Eurasia inferred from

satellite vegetation index data. *Journal of Geophysical Research*, **107,** 10.1029/2001JD001075.

BUERMANN, W., WANG, Y., DONG, J., ZHOU, L., ZENG, X., DICKINSON, R. E., POTTER, C. S., and MYNENI, R. B., 2002, Analysis of multi-year global vegetation leaf area index data set. *Journal of Geophysical Research*, **107**, 10.1029/2001JD000975.

CASPERSEN, J. P., PACALA, S. W., JENKINS, J. C., HURTT, G. C., MOORCROFT, P. R., and BIRDSEY, R. A., 2000, Contributions of land-use history to carbon accumulation in U.S. forests. *Science*, **290**, 1148–1151.

CAYAN, R. C., KAMMERDIENER, S. A., DETTINGER, M. D., CAPRIO, J. M., and PETERSON, D. H., 2001, Changes in the onset of spring in the western United States. *Bulletin of the American Meteorological Society*, **82**, 399–415.

CHINESE MINISTRY OF FORESTRY, 1988–1998, *China Forestry Statistics* (1949–1987, 1988, 1989, 1990, 1991, 1992, 1993, 1994, 1995, 1996, 1997) (Beijing: China Forestry Publishing House).

CHINESE MINISTRY OF FORESTRY, 1999–2001, *China Forestry Statistics Yearbook* (1998, 1999, 2000) (Beijing: China Forestry Publishing House).

COLOMBO, S. J., 1998, Climatic warming and its effect on bud burst and risk of frost damage to white spruce in Canada. *Forestry Chronicle*, **74**, 567–577.

DELUCIA, E. H., HAMILTON, J. G., NAIDU, S. L., THOMAS, R. B., ANDREWS, J. A., FINZI, A., LAVINE, M., MATAMALA, R., MOHAN, J. E., HENDREY, G. R., and SCHLESINGER, W. H., 1999, Net primary production of a forest ecosystem with experimental CO_2 enrichment. *Science*, **284**, 1177–1179.

FAN, S., GLOOR, M., MAHLMAN, J., PACALA, S., SARMIENTO, J., TAKAHASHI, T., and TANS, P., 1998, A large terrestrial carbon sink in North America implied by atmospheric and oceanic carbon dioxide data and models. *Science*, **282**, 442–446.

FITTER, A. H., and FITTER, R. S. R., 2002, Rapid changes in flowering time in British plants. *Science*, **296**, 1689.

FRIEDL, M. A., MCIVER, D. K., HODGES, J. C. F., ZHANG, X. Y., MUCHONEY, D., STRAHLER, A. H., WOODCOCK, C. E., GOPAL, S., SCHNEIDER, A., COOPER, A., BACCINI, A., GAO, F., and SCHAAF, C., 2002, Global land cover mapping from MODIS: algorithms and early results. *Remote Sensing of Environment*, **83**, 287–302.

GOODALE, C. L., APPS, M. J., BIRDSEY, R. A., FIELD, C. B., HEATH, L. S., HOUGHTON, R. A., JENKINS, J. C., KOHLMAIER, G. H., KURZ, W., LIU, S., NABUURS, G., NILSSON, S., and SHVIDENKO, A. Z., 2002, Forest carbon sinks in the northern hemisphere. *Ecological Applications*, **12**, 891–899.

GUTMAN, G. G., 1999, On the use of long-term global data of land reflectance and vegetation indices derived from the advanced very high resolution radiometer. *Journal of Geophysical Research*, **104**, 6241–6255.

HANSEN, J., RUEDY, R., GLASCOE, J., and SATO, M., 1999, GISS analysis of surface temperature change. *Journal of Geophysical Research*, **104**, 30997–31022.

HOUGHTON, R. A., HACKLER, J. L., and LAWRENCE, K. T., 1999, The U.S. carbon budget: contributions from land-use change. *Science*, **285**, 574–578.

HOUGHTON, R. A., HACKLER, J. L., and LAWRENCE, K. T., 2000, Changes in terrestrial carbon storage in the United States. 2: The role of fire and fire management. *Global Ecology & Biogeography*, **9**, 145–170.

IPCC, 2001, *Climate Change 2001: Synthesis Report. A Contribution of Working Groups I, II, and III to the Third Assessment Report of the Intergovernmental Panel on Climate Change*, edited by R. T. Watson and the Core Writing Team (Cambridge: Cambridge University Press).

JAMES, M. E., and KALLURI, S. N. V., 1994, The Pathfinder AVHRR land data set: an improved coarse-resolution data set for terrestrial monitoring. *International Journal of Remote Sensing*, **15**, 3347–3364.

KAUFMANN, R. K., ZHOU, L., KNYAZIKHIN, Y., SHABANOV, N. V., MYNENI, R. B., and TUCKER, C. J., 2000, Effect of orbital drift and sensor changes on the time series of AVHRR vegetation index data. *IEEE Transactions on Geoscience and Remote Sensing*, **38**, 2584–2597.

KEELING, C. D., CHIN, J. F. S., and WHORF, T. P., 1996, Increased activity of northern vegetation inferred from atmospheric CO_2 measurements. *Nature*, **382**, 146–149.

LIU, J., 1996, *A Macro Inventory of China's Environments and Resources and Their Dynamics* (Beijing: China's Scientific Publication House) [in Chinese].

LUCHT, W., PRENTICE, I. C., MYNENI, R. B., SITCH, S., FRIEDLINGSTEIN, P., CRAMER, W., BOUSQUET, P., BUERMANN, W., and SMITH, B., 2002, Climatic control of the high-latitude vegetation greening trend and Pinatubo effect. *Science*, **296**, 1687–1689.

MELILLO, J. M., MCGUIRE, A. D., KICKLIGHTER, D. W., MOORE, B., VOROSMARTY, C. J., and SCHLOSS, A. L., 1993, Global climate change and terrestrial net primary production. *Nature*, **363**, 234–240.

MINISTRY OF LAND AND RESOURCES OF CHINA, 2002, *Report of the 2001 National Survey of Land-use Change* (Beijing: China Land Press).

MYNENI, R. B., HALL, F. G., SELLERS, P. J., and MARSHAK, A. L., 1995, The interpretation of spectral vegetation indexes. *IEEE Transactions on Geoscience and Remote Sensing*, **33**, 481–486.

MYNENI, R. B., KEELING, C. D., TUCKER, C. J., ASRAR, G., and NEMANI, R. R., 1997a, Increased plant growth in the northern high latitudes from 1981 to 1991. *Nature*, **386**, 698–702.

MYNENI, R. B., NEMANI, R. R., and RUNNING, S., 1997b, Estimation of global leaf area index and absorbed PAR using radiative transfer models. *IEEE Transactions on Geoscience and Remote Sensing*, **35**, 1380–1393.

MYNENI, R. B., TUCKER, C. J., ASRAR, G., and KEELING, C. D., 1998, Interannual variations in satellite-sensed vegetation index data from 1981 to 1991. *Journal of Geophysical Research*, **103**, 6145–6160.

MYNENI, R. B., DONG, J., TUCKER, C. J., KAUFMANN, R. K., KAUPPI, P. E., LISKI, J., ZHOU, L., ALEXEYEV, V., and HUGHES, M. K., 2001, A large carbon sink in the woody biomass of northern forests. *Proceedings of the National Academy of Sciences of the United States of America*, **98**, 14784–14789.

NADELHOFFER, K. J., EMMETT, B. A., GUNDERSEN, P., KJONAAS, O. J., KOOPMANS, C. J., SCHLEPPI, P., TIETEMA, A., and WRIGHT, R. F., 1999, Nitrogen deposition makes a minor contribution to carbon sequestration in temperate forests. *Nature*, **398**, 145–148.

NEMANI, R., WHITE, M., THORNTON, P., NISHIDA, K., REDDY, S., JENKINS, J., and RUNNING, S., 2002, Recent trends in hydrologic balance have enhanced the terrestrial carbon sink in the United States. *Geophysical Research Letters*, **29**, 10.1029/2002GL014867.

NEMANI, R. R., KEELING, C. D., HASHIMOTO, H., JOLLY, W. M., PIPER, S. C., TUCKER, C. J., MYNENI, R. B., and RUNNING, S. W., 2003, Climate-driven increases in global terrestrial net primary production from 1982 to 1999. *Science*, **300**, 1560–1563.

NEW, M., HULME, M., and JONES, P. D., 2000, Global Monthly Climatology for the Twentieth Century (New *et al.*). Data set. Available online (http://www.daac.ornl.gov) from Oak Ridge National Laboratory Distributed Active Archive Center, Oak Ridge, Tennessee, USA.

RANDERSON, J. T., FIELD, C. B., FUNG, I. Y., and TANS, P. P., 1999, Increases in early season ecosystem uptake explain recent changes in the seasonal cycle of atmospheric CO_2 at high northern latitudes. *Geophysical Research Letters*, **26**, 2765–2769.

SCHIMEL, D. S., ALVES, D., ENTING, I., HIMANN, M., JOOS, F., RAYNAUD, D., and WIGLEY, T., 1996, CO_2 and the carbon cycle. In *Climate Change 1995: The Science of Climate Change*, edited by J. T. Houghton, L. G. Meira Filho, B. A. Callender, N. Harris, A. Kattenberg and K. Maskell (New York: Cambridge University Press), pp. 76–86.

SCHIMEL, D. S., MELILLO, J., TIAN, H., MCGUIRE, A. D., KICKLIGHTER, D., KITTEL, T., ROSENBLOOM, N., RUNNING, S., THORNTON, P., OJIMA, D., PARTON, W., KELLY, R., SYKES, M., NEILSON, R., and RIZZO, B., 2000, Contribution of increasing CO_2 and climate to carbon storage by ecosystems in the United States. *Science*, **287**, 2004–2006.

SCHIMEL, D. S., HOUSE, J. I., HIBBARD, K. A., BOUSQUET, P., CIAIS, P., PEYLIN, P., BRASWELL, B. H., APPS, M. J., BAKER, D., BONDEAU, A., CANADELL, J., CHURKINA, G., CRAMER, W., DENNING, A. S., FIELD, C. B., FRIEDLINGSTEIN, P., GOODALE, C., HEIMANN, M., HOUGHTON, R. A., MELILLO, J. M., MOORE, B., MURDIYARSO, D., NOBLE, I., PACALA, S. W., PRENTICE, I. C., RAUPACH, M. R., RAYNER, P. J., SCHOLES, R. J., STEFFEN, W. L., and WIRTH, C., 2001, Recent patterns and mechanisms of carbon exchange by terrestrial ecosystems. *Nature*, **414**, 169–172.

SHEN, D., and VARIS, O., 2001, Climate change in China. *Ambio*, **30**, 381–383.

SLAYBACK, D. A., PINZON, J. E., LOS, S. O., and TUCKER, C. J., 2003, Northern hemisphere photosynthetic trends 1982–99. *Global Change Biology*, **9**, 1–15.

TIAN, H., MELILLO, J. M., KICKLIGHTER, D. W., McGUIRE, A. D., HELFRICH III, J. V. K., MOORE III, B., and VÖRÖSMARTY, C. J., 1998, Effect of interannual climate variability on carbon storage in Amazon ecosystems. *Nature*, **396**, 664–667.

TANS, P. P., FUNG, I. Y., and TAKAHASHI, T., 1990, Observation constraints on the global atmospheric CO_2 budget. *Science*, **247**, 1431–1438.

TONG, C., HALL, C. A. S., and WANG, H., 2003, Land use change in rice, wheat and maize production in China (1961–1998). *Agriculture, Ecosystems and Environment*, **95**, 523–536.

TUCKER, C. J., SLAYBACK, D. A., PINZON, J. E., LOS, S. O., MYNENI, R. B., and TAYLOR, M. G., 2001, Higher northern latitude normalized difference vegetation index and growing season trends from 1982 to 1999. *International Journal of Biometeorology*, **45**, 184–190.

VAN AUKEN, O. W., 2000, Shrub invasions of North American semiarid grasslands. *Annual Review of Ecology and Systematics*, **31**, 197–215.

WORLD RESOURCES INSTITUTE, 1994, *World Resources 1994–1995* (Oxford: Oxford University).

ZHAI, P., SUN, A., REN, F., LIU, X., GAO, B., and ZHANG, Q., 1999, Changes of climate extremes in China. *Climatic Change*, **42**, 203–218.

ZHANG, P., ZHOU, X., and WANG, F., 1999, *Introduction to Natural Forest Conservation Program* (Beijing: China's Forestry Publishing House) [in Chinese].

ZHANG, P., SHAO, G., ZHAO, G., LE MASTER, D. C., PARKER, G. R., DUNNING, J. B., and LI, Q., 2000, Ecology—China's forest policy for the 21st century. *Science*, **288**, 2135–2136.

ZHOU, L., TUCKER, C. J., KAUFMANN, R. K., SLAYBACK, D., SHABANOV, N. V., and MYNENI, R. B., 2001, Variations in northern vegetation activity inferred from satellite data of vegetation index during 1981 to 1999. *Journal of Geophysical Research*, **106**, 20069–20083.